

Simple model for laser-induced electron dynamics

R. Gómez-Abal and W. Hübner

Max-Planck Institut für Mikrostrukturphysik Weinberg 2, D-06120, Halle, Germany

(Received 18 July 2001; revised manuscript received 12 December 2001; published 26 April 2002)

As a first step to address the recently observed ultrafast dynamics in ferromagnetic metals we analyze a simple model employing two- and three-level systems. We calculate the electron dynamics of the systems for a variety of laser-pulse durations and intensities. The model is sufficiently flexible to handle the laser manipulation of population and phase dynamics on femtosecond time scales. For the three-level system, it allows us to describe the phase control of the different optical excitation paths.

DOI: 10.1103/PhysRevB.65.195114

PACS number(s): 78.47.+p, 78.20.Bh, 32.80.Qk

I. INTRODUCTION

The development of ultrashort (femtosecond) laser pulses has given the experimentalists the opportunity to measure the dynamic behavior of quantum systems with very high time resolution. While laser manipulation is already well understood in atomic and molecular systems, device applications demand for an implementation of these mechanisms in a solid-state environment. Thus, the investigation of electron and spin dynamics in the bulk, surfaces, and nanostructures of nonmagnetic as well as magnetic metals and semiconductors has recently started to attract considerable interest. Already in 1987, the transient reflection measurements by Schoenlein *et al.*¹ showed that a nonequilibrium electron distribution in Au could be obtained within less than 1 ps, and that this distribution relaxed by thermalization to the lattice within 2–3 ps.

Later, the photoemission measurements by Fann *et al.*² demonstrated that there is a finite relaxation time of the electrons from their nascent to the Fermi-Dirac distribution. Sun *et al.*³ were able to fit their transient reflectivity measurements with a thermalization time for the electron gas of the order of 500 fs.

Time-resolved two-photon photoemission investigations on Cu(111) surfaces using 60-fs laser pulses, performed by Hertel *et al.*⁴ showed that the time it takes the electron distribution to reach the maximum energy absorption, commonly identified with the thermalization of the electron subsystem, ranges from less than 10 fs to about 300 fs depending on the photon energy. A dephasing time of ≈ 20 fs was measured one year later by Ogawa *et al.*⁵ Also the lifetime of image states on Cu(100) surfaces has been investigated by two-photon photoemission. Values ranging from 40 fs to 300 fs depending on the distance of these states from the surface have been reported.⁶ Time-resolved two-photon photoemission also revealed a lifetime of the optically excited states in Pt_3^- of less than 70 fs.⁷

The same ultrafast dynamics of the nascent electron distribution has been observed in semiconductors. Dephasing times of the order of 20 fs have been observed for oxide-covered GaAs(100) surfaces⁸ and less than 100 fs for Si,^{9,10} while the carrier relaxation times were measured, ranging from 20 fs to more than 400 fs for GaAs¹¹ and from 200 fs up to 1200 fs for Si.^{9,12} Likewise, measurements of the

surface-plasmon resonance (in the frequency domain)¹³ as well as time-resolved pump-probe experiments¹⁴ on metal nanoparticles embedded in a glass matrix showed relaxation times ranging from several femtoseconds up to a few picoseconds. Direct femtosecond-time-resolved measurements of the plasmon decay time with values of 2–9 fs in metal nanoparticle gratings were recently performed by Lamprecht *et al.*¹⁵ on gold nanoparticle arrays produced by electron-beam lithography.

Recent pump-probe experiments have shown fast demagnetization processes occurring on the femtosecond time scale.^{16–20} This ultrafast dynamics, much faster than the usual spin-lattice relaxation that is of the order of nanoseconds, is of quantum-mechanical nature and their theoretical investigation demands the solution of the time-dependent Schrödinger equation. Such a calculation has already been performed for Ni, showing that charge and spin dynamics occur within the first 20 fs.²¹

These interesting phenomena have opened up new lines of research. One of them is the possibility to control the quantum state of a system. This could trigger a new technological development in quantum computing as well as in optical recording. In order to achieve these technological applications it is necessary to control the dynamics of the electronic system so that one can change its state back and forth.

This kind of processes is nowadays the target of many research groups, and many interesting results have already been obtained, showing the importance of the relative phases of the quantum system, the pulse shape, and the time delay between pulses.^{22–27}

To explore the possibility of coherent control by ultrashort laser pulses within a simple model, well known in molecular physics but prototypic for surfaces and gap states in solids, we start with the electron dynamics of two-level and three-level systems. The interaction of a system with a strong, rapidly varying electromagnetic pulse, during a very short time, requires a full nonadiabatic treatment of the problem. Only nondiagonal elements are considered in the interaction with the field, which is correct if the angular momentum of the electrons is a good quantum number. The dynamical Stark effect can be observed within these approximations. The changes in the level energies, due to the change in the Coulomb interaction coming from the nonequilibrium elec-

tron distribution are not included. Within this model, the coherent dephasing due to the different time evolution of states with different energies is included. We do not include incoherent dephasing (as a transversal decay time $-T_2$) since it corresponds to thermodynamical properties that go beyond the scope of our work.

We show that the optoelectronic switching process can be performed on the femtosecond time scale. We also address the dependence of the system response to the variations of the laser-pulse parameters (i.e., frequency, amplitude, pulse duration, and shape). We show the importance of the relative quantum phase of the electronic wave functions in obtaining a desired final state, which leads to the outline of a possible quantum-optical recording device.

II. THEORY

The model Hamiltonian has the form

$$H(x,t) = H_0(x) + V(x,t), \quad (1)$$

where H_0 is the time-independent Hamiltonian of the electronic system and $V(x,t)$ is the interaction of the electronic system with the electromagnetic field, for which we consider only the electric dipolar term.

Since we are interested in the response of the system to the application of several laser pulses and, experimentally, these pulses are not isolated but periodically repeated, we simulate the laser by a periodically applied pulse.

This periodicity allows us to use numerical methods specially designed for these cases. In order to study this kind of processes, it is necessary to solve the time-dependent Schrödinger equation

$$H(x,t)\psi(x,t) = i\hbar \frac{\partial}{\partial t} \psi(x,t). \quad (2)$$

The quantum states evolve in time according to

$$\psi(t) = U(t,0)\psi(0), \quad (3)$$

where $U(t,0)$ is the time-evolution operator, obeying the equation

$$\frac{d}{dt}U(t,0) = -\frac{i}{\hbar}H(t)U(t,0). \quad (4)$$

The density operator of the system, which is initially equal to $\rho(0)$, evolves in time according to

$$\rho(t) = U(t,0)\rho(0)U^\dagger(t,0), \quad (5)$$

where U^\dagger denotes the adjoint of U . The treatment of the quantum evolution within the density-matrix formalism allows us to include the relaxation in simplified models, like that of the relaxation-time approximation. This is not done in our case since we want to keep a full quantum-mechanical treatment of the electronic system.

To calculate this operator, we perform a direct time-domain integration in one period as follows:²⁸ we divide the

modulation period into N equally spaced segments, then the propagator u_j of the j th time interval is calculated numerically by

$$u_j = U[j\Delta t, (j-1)\Delta t] = \exp\left(-\frac{i}{\hbar} \int_{(j-1)\Delta t}^{j\Delta t} H(t)dt\right) \quad (6)$$

$$1 \leq j \leq N.$$

The accumulated propagators U_j over j segments are calculated by the recursion

$$U_j = U(j\Delta t, 0) = u_j U_{j-1}, \quad 1 \leq j \leq N, \quad (7)$$

with the initial condition $U_0 = 1$. For the time evolution within the k th period, we have

$$U[(k-1)T + (jt, 0)] = U_{(k-1)N+j} = (U_N)^{k-1} U_j. \quad (8)$$

Because of the time periodicity of the problem, we have alternatively used the Floquet-matrix method that is especially suited for periodic problems. We are interested in facing simultaneously and on the same footing, different time scales, i.e., pulses whose main frequency and width are in the femtosecond range and a repetition period between them of the order of several nanoseconds. In such cases, many harmonic frequencies are needed for a successful description of the pulse, and the size of the Floquet matrix needed to get converged results makes this method very cumbersome and inefficient compared with what we get by using the direct time-domain integration algorithm. We always found that the direct time-domain integration of the Schrödinger equation is more efficient even for unrealistic repetition times of the order of picoseconds.

III. TIME VERSUS FREQUENCY DOMAIN CALCULATIONS

Before starting with the results of the interaction of a laser pulse with a quantum system, let us compare the computational efficiencies of the frequency domain and direct time-domain integration. This analysis is based on that of Ref. 28. We also make the assumption that the number of floating point operations (flops) determines the computational time.

Diagonalization of a general $N \times N$ matrix approximately involves $3N^3$ flops, while calculating the product of two matrices of the same dimension requires $2N^3$ operations. Evaluation of transcendental functions is empirically found to require about 10 flops.

For the Floquet-matrix algorithm, one must truncate the Floquet matrix. That is made, as usual, in two ways; by taking a finite number of basis functions ϕ_j for the unperturbed Hamiltonian H_0 as well as by limiting the number of harmonics in the Fourier expansion of the time dependence. If \mathcal{N} is the number of basis functions and m the number of terms for the Fourier expansion, then, usually the size of the matrix taken is $nm\mathcal{N}$ where n is a small integer (value around 5). The number of flops required to diagonalize the Floquet matrix is then approximately

$$N_{Floquet} \approx 3n^3 m^3 \mathcal{N}^3. \quad (9)$$

For the integration in the time domain (td) one must diagonalize the Hamiltonian, the size of which is \mathcal{N} , for each time interval (that means $3\mathcal{N}^3$ flops per interval), and also the evaluation of a transcendental function for each eigenvalue of the Hamiltonian [to solve Eq. (6) adding another $10\mathcal{N}$ flops per interval]. Each time step also includes at least five matrix multiplications, two for taking the time-evolution operator in one time interval to the original basis, one to generate the accumulated propagator and two more to evaluate the time-dependent density matrix, (that adds another $10\mathcal{N}^3$). If we take n_T as the number of time intervals over one period, the number of flops required is then approximately

$$N_{td} \approx n_T 3\mathcal{N}^3 + n_T 10\mathcal{N}^3 + n_p n_T 2\mathcal{N}^3 = (13 + 2n_p)n_T \mathcal{N}^3. \quad (10)$$

The first term in the upper right part represents the number of flops needed for diagonalization, the second is the number of flops needed for matrix multiplications for the first period, and the third is the number of flops needed for the calculation of the time evolution during another n_p periods. Since once the time evolution is known in the first period, its calculation for the next ones requires only one matrix multiplication per time interval. We have not included terms linear in \mathcal{N} since they will be less important as the number of states taken into account grow.

To obtain the same precision, the number of time intervals in the time-domain integration and the cutoff in the Fourier expansion in Floquet algorithm should be proportional. $n_T \approx 2m$ is usually a good selection. Taking this into account, the relation between the different methods is

$$\frac{N_{Floquet}}{N_{td}} = \frac{3n^3 n_T^2}{2(13 + 2n_p)}. \quad (11)$$

For example, we want to calculate the time evolution of the system for a pulse of 20 fs full width at half maximum (FWHM) with a main frequency corresponding to 1 eV. The corresponding frequency for 1 eV is $\omega \approx 1.5 \times 10^3$ THz, which corresponds to an oscillation period of around 4 fs. Then, a time interval of 0.1 fs should give a good numerical precision. If the time between pulses is of the order of 1 ps, which is already unrealistic when taking into account that experimentally the time between two pulses is of the order of several nanoseconds, the number of time steps is $n_T = 10^4$. Taking as an example, $n = 5$ and a calculation of ten periods ($n_p = 10$), the resulting coefficient is around 5×10^8 , which means that the Floquet-matrix method is eight orders of magnitude more *expensive*. Because with the values of n_p and n selected, the quotient is approximately $5.7n_T^2$, there are no values of n_T for which the Floquet-matrix method should be more efficient.

This means that, unless the time-dependent perturbation can be expanded in only a few Fourier coefficients, the use of the Floquet-matrix method is not recommendable and it is not useful in any case for our interest.

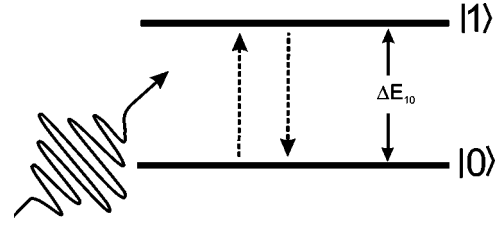


FIG. 1. Two-level scheme.

IV. RESULTS

We start our investigations of the electron dynamics with the simplest nontrivial case of a quantum system, a two-level atom excited by a laser pulse that connects both levels, as shown in Fig. 1. The energy difference ΔE_{10} between the levels $|1\rangle$ and $|0\rangle$ is 1 eV. We revisit these results, already known from optics, for two different pulse shapes, Gaussian shaped [$I(t) \propto \exp(-t^2/\sigma^2)$] and sech^2 shaped [$I(t) \propto \text{sech}^2(t/\sigma)$], as shown in Fig. 2. We can then analyze the influence of the pulse shape on the behavior of the system. At this point it is important to mention the work of Mukamel and Jortner²⁹ explaining the experimental results of Williams *et al.*³⁰ There they show that in resonance, the decay of the electronic state depends only on the lifetime of the excited states, which in our case is infinite. However, out of resonance, the decay time of the laser pulse is dominating, which we have also observed. The zero occupation after the pulse, when it is out of resonance, is due to the decay of the occupation as the pulse is turned off.

The dependence of the occupation of the excited state $|1\rangle$ as a function of the main frequency of the pulse is shown in Fig. 3 for an arbitrary maximum amplitude and width, but the same for both pulse shapes. It can be observed that the occupation of the excited state reaches a maximum when the main frequency of the pulse is in resonance with the energy difference ΔE_{10} between the two states irrespective of the pulse shape. The latter one just affects the pulse duration at which a complete transition to the excited state occurs. In Fig. 3 the width of the pulses is such that only the sech^2 -shaped one gives a complete transition. Once this fre-

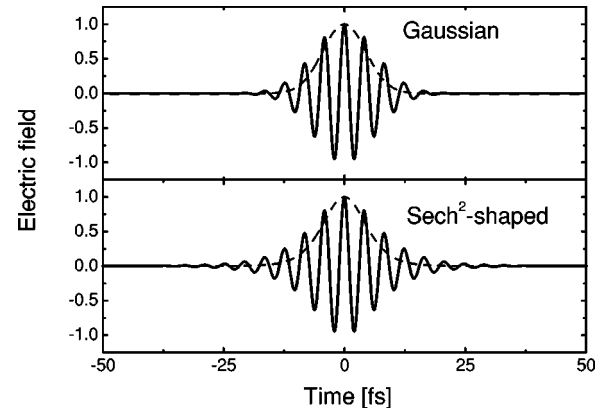


FIG. 2. Real part (solid line) and intensity (dashed line) of the electric field as a function of time for a (a) Gaussian and (b) sech^2 -shaped laser pulse.

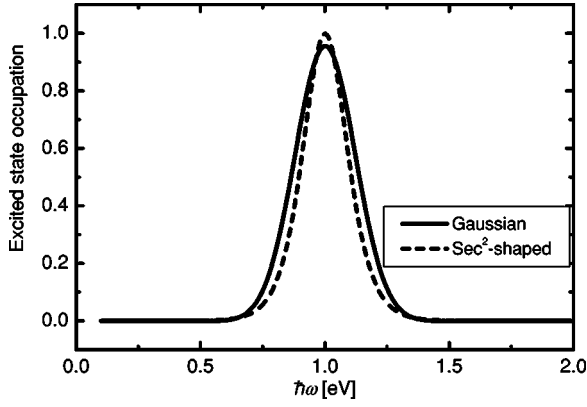


FIG. 3. Occupation of the excited state ($|1\rangle$) as a function of the main frequency of the pulse.

quency is tuned, we are in a position to analyze the dependence on other parameters, such as the pulse width or intensity.

Figure 4 shows the dependence of the occupation of the excited state (shading) on both the electric-field amplitude (y axis)³¹ and the pulse duration, measured by its temporal FWHM (x axis), for a main frequency resonant with the level splitting and a sech^2 -shaped pulse. Alternate zones of high (black) and low (white) occupation for both constant $|\vec{p} \cdot \vec{E}|$ or constant FWHM can be observed. The dashed contour lines in Fig. 4 correspond to a constant value of the product of pulse duration and electric-field amplitude. It is clear that this product is the quantity that must be tuned to obtain the complete transition to the excited state, and not the total energy of the pulse, which is proportional to the field intensity that is the square of the field amplitude. Shorter pulses dump less energy to the sample and nevertheless yield the same result.

Figure 5 shows a horizontal cut of Fig. 4 at (a) $|\vec{p} \cdot \vec{E}| = 0.05$ eV and (b) $|\vec{p} \cdot \vec{E}| = 0.1$ eV (marked by the arrows on both sides of the graph in Fig. 4) and also for the Gaussian pulses. The oscillatory behavior is clearly visible, and the

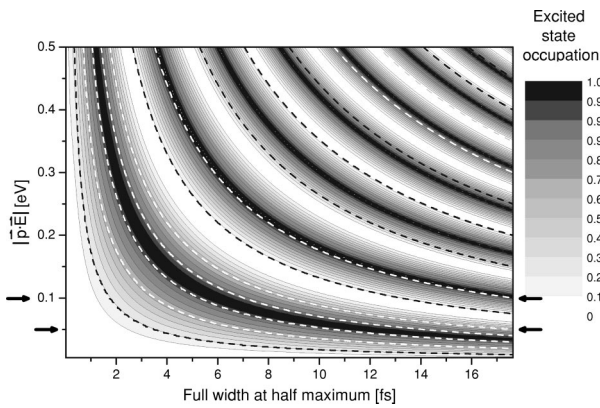


FIG. 4. Occupation of the excited state (shading) on both the electric-field amplitude (y axis) and the pulse duration (x axis), for a main frequency resonant with the level splitting and a sech^2 -shaped pulse. The dashed lines correspond to $\text{FWHM} \cdot |\vec{E}| = \text{const}$ (FWHM means temporal full width at half maximum).

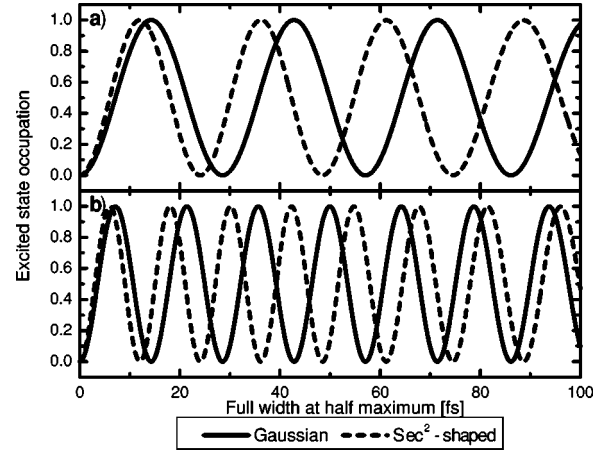


FIG. 5. Occupation of the excited state as a function of the pulse width for (a) $|\vec{p} \cdot \vec{E}| = 0.05$ eV and (b) $|\vec{p} \cdot \vec{E}| = 0.1$ eV.

only difference between the different pulse shapes is the different frequency of this oscillation. This behavior is related to the occurrence of Rabi oscillations during the pulse. The frequency difference factor of 2 between (a) and (b) is due to doubling of the maximum electric-field amplitude. The slightly different frequency obtained as a function of the pulse width for different pulse shapes is due to the fact that for the same peak fluence, which in the cases shown corresponds approximately to (a) $6.5 \times 10^{11} (\text{W}/\text{m}^2)$ and (b) $2.6 \times 10^{12} (\text{W}/\text{m}^2)$, respectively, the total energy density is different for the sech^2 -shaped and the Gaussian pulse. For the same FWHM, the sech^2 -shaped pulse energy transfer is approximately 1.07 times the one for the Gaussian pulse.

Figure 6(a) shows the time evolution of the level occupation for a Gaussian pulse, when the conditions for a complete transition are fulfilled, that is, the duration of the pulse, for fixed pulse shape and amplitude, is properly tuned. The cases shown in Figs. 6(b) and 6(c) correspond to widths of the

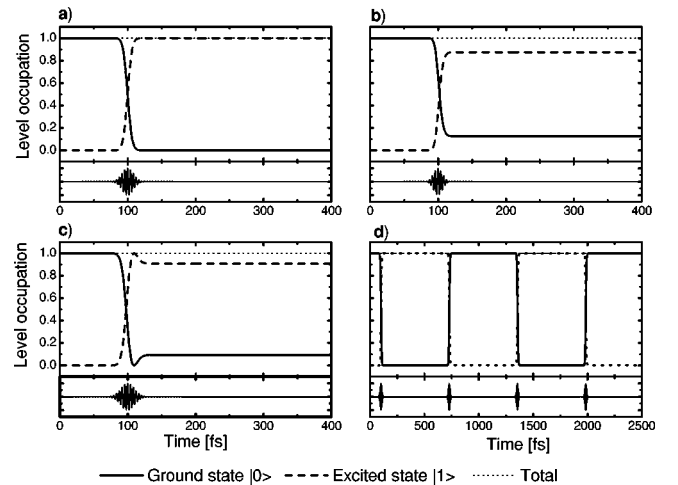


FIG. 6. Time evolution of the occupation for a two-level system excited by a Gaussian pulse. (a) Total transition, (b) underexcitation, (c) overexcitation, and (d) several pulses tuned to total transition.

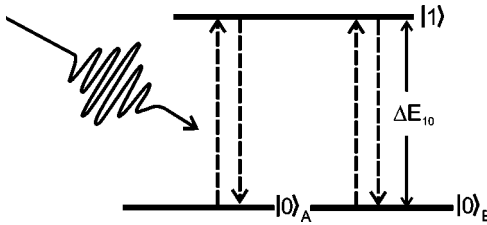


FIG. 7. Three-level scheme.

pulses being too short or too long, respectively. In the first case, the excitation is turned off before the system reaches a transition probability equal to one, while in the second, the pulse is still on when the complete transition is obtained thus generating stimulated emission that begins to take the system again to its ground state.

As can be seen in Fig. 6(d) the successive application of pulses makes the system go from the ground state to the excited state and back, so that in this system it is easily possible to control the state of the system and make it work as a read/write unit. The absence of damping in the Hamiltonian, makes it stay at the excited state forever. In the figure, the time delay between pulses is 0.7 ps, and the same result is obtained for longer or shorter (as far as the pulses do not overlap) time delays. The figures show that the dynamics occurs only during the application of the pulse. Nothing happens afterwards, due to the absence of damping in our model. The maintenance of the total occupation serves as a test for the precision of our calculation. No qualitative difference can be observed for sech^2 -shaped pulses.

Next we turn our attention to the three-level system as shown in Fig. 7. In this case we have a new free parameter, the energy position of the third level, which we keep fixed at zero energy. We analyze the particular case in which the ground state is doubly degenerate, as shown in Fig. 7. As in the two-level system, $\Delta E_{10} = 1$ eV. We start with the electron in one of these two states. After the application of the pulse, we obtain a total transition from one to the other ground state. As can be seen in Fig. 8(a), the laser pulse stimulates the transition from the occupied state to the excited one, and as soon as this state begins to get populated, the laser also induces the transition from this state to the other ground state.

The question posed by this result is: Why does it exclusively go to the unoccupied state, and not to both the ground states with equal probability? To understand this effect, we take a snapshot at the moment when both ground states have the same occupation (0.25) and the excited state 0.5. From this point of view, both ground states are symmetric, so the electron could, in principle, decay to any of them. The only difference between them is their relative phases.

If, at this point, we exchange the phase of the two ground states, as shown in Fig. 8(b), the system goes back to the original state, and, if we force both phases to be equal [Fig. 8(c)] then the states cannot be distinguished and the electron has the same probability of going to any of them. These important results show that the path followed by the transition is determined by the relative phase of the wave functions. Moreover, the transition shown in Fig. 8(a) is the only

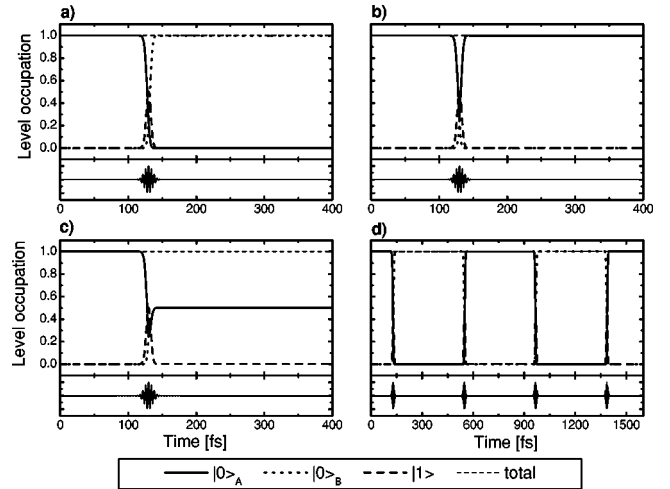


FIG. 8. Time evolution of the occupation of the three-level system and its dependence on the relative phase of the wave functions.

one obtained, unless we change the phases “by hand.” The existence of two ground states should only be possible if these two states have different symmetry properties. The ability to measure this property if, for example, the two levels had different spins, could make this system an ideal one for magneto-optical storage. Since in both states the system is in its ground state, it should stay there for very long times if, for example, the transition between the two ground states takes place only through tunneling. Also, after writing, there is no energy stored in the system, all the energy absorbed when going from one ground state to the excited state is completely reemitted when decaying to the other ground state. And, as can be seen in Fig. 8(d), the application of a second pulse takes the system back to its original ground state.

V. CONCLUSIONS

We have shown that the dynamics of electrons interacting with an electromagnetic field can be successfully addressed, and also confirmed that this may happen within femtoseconds. We have also shown that the Floquet-matrix method is quite inefficient to treat this kind of problem compared to the direct time integration we use.

The control of the transitions in the two-level system from one state to another and back can be obtained. To obtain a complete transition, it is necessary to tune the duration of the laser pulse, as well as its frequency and amplitude. Different pulse shapes give qualitatively the same behavior.

We also want to point out the importance of the relative phase in the quantum state, which can define the path of transitions in the population dynamics of many-level systems. In three-level systems, the additional degree of freedom is important for a solid-state implementation of fast optical switching. This task, as well as other interesting coherent phenomena in solids will be addressed in a forthcoming publication.

- ¹R. W. Schoenlein, W. Z. Lin, J. G. Fujimoto, and G. L. Eesley, *Phys. Rev. Lett.* **58**, 1680 (1987).
- ²W. S. Fann, R. Storz, H. W. K. Tom, and J. Bokor, *Phys. Rev. Lett.* **68**, 2834 (1992).
- ³C.-K. Sun, F. Vallée, L. H. Acioli, E. P. Ippen, and J. G. Fujimoto, *Phys. Rev. B* **50**, 15 337 (1994).
- ⁴T. Hertel, E. Knoesel, M. Wolf, and G. Ertl, *Phys. Rev. Lett.* **76**, 535 (1996).
- ⁵S. Ogawa, H. Nagano, H. Petek, and A. P. Heberle, *Phys. Rev. Lett.* **78**, 1339 (1997).
- ⁶U. Höfer, I. L. Shumay, U. Thomann, W. Wallauer, and Th. Fauster, *Science* **279**, 190 (1998).
- ⁷N. Pontius, P. S. Bechthold, M. Neeb, and W. Eberhardt, *Phys. Rev. Lett.* **84**, 1132 (2000).
- ⁸H. W. K. Tom, Y. M. Chang, and H. Kwak, *Appl. Phys. B: Lasers Opt.* **68**, 305 (1999).
- ⁹T. Sjödin, C.-M. Li, H. Petek, and H.-L. Dai, *Chem. Phys.* **251**, 205 (2000).
- ¹⁰J. R. Goldman and J. A. Prybyla, *Phys. Rev. Lett.* **72**, 1364 (1994).
- ¹¹C. A. Schmuttenmaer, C. Cameron Miller, J. W. Herman, J. Cao, D. A. Mantell, Y. Gao, and R. J. D. Miller, *Chem. Phys.* **205**, 91 (1996).
- ¹²Note that the values of both dephasing and charge relaxation times are smaller for GaAs than for Si. The difference is due to the fact that the gap is direct in GaAs while it is indirect in Si. Optical phonons are present in both materials.
- ¹³N. Del Fatti, F. Vallée, C. Flytzanis, Y. Hamanaka, and A. Nakamura, *Chem. Phys.* **251**, 215 (2000).
- ¹⁴J.-Y. Bigot, V. Halté, J.-C. Merle, and A. Daunois, *Chem. Phys.* **251**, 181 (2000).
- ¹⁵B. Lamprecht, G. Schider, R. T. Lechner, H. Ditlbacher, J. Krenn, A. Leitner, and F. R. Aussenegg, *Phys. Rev. Lett.* **84**, 4721 (2000).
- ¹⁶A. Scholl, L. Baumgarten, R. Jacquemin, and W. Eberhardt, *Phys. Rev. Lett.* **79**, 5146 (1997).
- ¹⁷B. Koopmans, M. van Kampen, J. T. Kohlhepp, and W. J. M. de Jonge, *Phys. Rev. Lett.* **85**, 844 (2000).
- ¹⁸E. Beaurepaire, J.-C. Merle, A. Daunois, and J.-Y. Bigot, *Phys. Rev. Lett.* **76**, 4250 (1996).
- ¹⁹J. Hohlfeld, E. Matthias, R. Knorren, and K. H. Bennemann, *Phys. Rev. Lett.* **78**, 4861 (1997).
- ²⁰M. Aeschlimann, M. Bauer, S. Pawlik, W. Weber, R. Burgermeister, D. Oberli, and H. C. Siegmann, *Phys. Rev. Lett.* **79**, 5158 (1997).
- ²¹W. Hübner and G. P. Zhang, *Phys. Rev. B* **58**, R5920 (1998).
- ²²X. Marie, P. Le Jeune, T. Amand, M. Brousseau, J. Barrau, and M. Paillard, *Phys. Rev. Lett.* **79**, 3222 (1997).
- ²³J. M. Faser, A. I. Shkrebtii, J. E. Sipe, and H. M. van Driel, *Physica B* **272**, 353 (1999).
- ²⁴N. Garro, S. P. Kennedy, M. J. Snelling, R. T. Phillips, and K. H. Ploog, *Physica B* **272**, 371 (1999).
- ²⁵N. H. Bonadeo, J. Erland, D. Gammon, D. Park, D. S. Katzer, and D. G. Steel, *Science* **282**, 147 (1998).
- ²⁶V. Blanchet, C. Nicole, M.-A. Bouchene, and B. Girard, *Phys. Rev. Lett.* **78**, 2716 (1997).
- ²⁷A. Hartmann, Y. Ducommun, E. Kapon, U. Hohenester, and E. Molinari, *Phys. Rev. Lett.* **84**, 5648 (2000).
- ²⁸This algorithm is just the same as the first steps of the so-called *compute* algorithm [M. Edén, Y. K. Lee, and M. Levitt, *J. Magn. Reson. A* **120**, 56 (1996)], but we do not use it in the frequency space, since, up to now we are only interested in the time evolution, without looking on the spectra.
- ²⁹S. Mukamel and J. Jortner, *J. Chem. Phys.* **62**, 3609 (1975).
- ³⁰P. F. Williams, D. L. Rousseau, and S. H. Dworketsky, *Phys. Rev. Lett.* **32**, 196 (1974).
- ³¹ \vec{p} is the electric-dipole operator, its value is supposed to be constant through all the calculations. It is included in the axis label so that the marks have energy units, but the only quantity that changes is the electric-field amplitude of the laser pulse. If we take the value of $|\vec{p}|=1 \text{ eÅ}$ and $|\vec{p}\cdot\vec{E}|=0.1 \text{ eV}$, the corresponding peak fluence is $I=2.6\times 10^{12}(W/m^2)$.